Long-distance electron transport in individual, living cable bacteria

Bjerg, Jesper T.; Boschker, Henricus T.S.; Larsen, Steffen; Berry, David; Schmid, Markus; Millo, Diego; Tataru, Paula; Meysman, Filip J.R.; Wagner, Michael; Nielsen, Lars Peter

DOI
10.1073/pnas.1800367115

Publication date
2018

Document Version
Accepted author manuscript

Published in
Proceedings of the National Academy of Sciences of the United States of America

Citation (APA)
Bjerg, J. T., Boschker, H. T. S., Larsen, S., Berry, D., Schmid, M., Millo, D., Tataru, P., Meysman, F. J. R., Wagner, M., Nielsen, L. P., & Schramm, A. (2018). Long-distance electron transport in individual, living cable bacteria. *Proceedings of the National Academy of Sciences of the United States of America*, *115*(22), 5786-5791. https://doi.org/10.1073/pnas.1800367115

Title Page.

Classification: Biological Sciences, Microbiology

Title: Long-distance electron transport in individual, living cable bacteria

Short title: Long-distance electron transport in cable bacteria

Authors:

Jesper T. Bjerg[1,2*], Henricus T.S. Boschker[3,4], Steffen Larsen[2], David Berry[5,6], Markus Schmid[5,6], Diego Millo[7], Paula Tataru[8], Filip J. R. Meysman[4,3], Michael Wagner[5,6], Lars Peter Nielsen[1,2], and Andreas Schramm[1,2*]

Affiliations:

[1] Center for Electromicrobiology, Aarhus University, Ny Munkegade 114, DK-8000, Aarhus C, Denmark.

[2] Center for Geomicrobiology, Section for Microbiology, Department of Bioscience, Aarhus University, Ny Munkegade 114, DK-8000, Aarhus C, Denmark.

[3] Department of Biotechnology, Delft University of Technology, 2629 HZ Delft, The Netherlands

[4] Ecosystem Management Research Group, Department of Biology, University of Antwerp, BE- 2610 Wilrijk (Antwerp), Belgium

[5] Division of Microbial Ecology, Department of Microbiology and Ecosystem Science, University of Vienna, A-1090 Vienna, Austria.

[6] Research Network Chemistry meets Microbiology, University of Vienna, A-1090 Vienna, Austria

[7] Department of Physics and Astronomy, VU University Amsterdam, 1081 HV Amsterdam, The Netherlands

[8] Bioinformatics Research Centre, Aarhus University, DK-8000, Aarhus C, Denmark.

***Correspondence:** jjbjerg@bios.au.dk - +45 40433087 or andreas.schramm@bios.au.dk - +45 60202659

Keywords: *Electromicrobiology, Raman spectroscopy, Cytochrome C, Cable bacteria*

Abstract.

Electron transport within living cells is essential for energy conservation in all respiring and photosynthetic organisms. While a few bacteria transport electrons over µm-distances to their surroundings, filaments of cable bacteria are hypothesized to conduct electric currents over cm-distances. We used resonance Raman microscopy to analyze cytochrome redox states in living cable bacteria. Cable bacteria filaments were placed in microscope chambers with sulfide as electron source and oxygen as electron sink at opposite ends. Along individual filaments a gradient in cytochrome redox potential was detected, which immediately broke down upon removal of oxygen or laser-cutting of the filaments. Without access to oxygen, a rapid shift towards more reduced cytochromes was observed, as electrons were no longer drained from the filament but accumulated in the cellular cytochromes. These results provide the first direct evidence for long-distance electron transport in living multicellular bacteria.

Significance Statement.

Cable bacteria are cm-long, multicellular filamentous bacteria, which are globally occurring in marine and freshwater sediments. Their presence coincides with the occurrence of electrical fields, and gradients of oxygen and sulfide that are best explained by electron transport from sulfide to oxygen along the cable bacteria filaments, implying electric conductance by living bacteria over cm-distances. Until now, all indications for such long-distance electron transport were derived from bulk sediment incubations. Here we for the first time present measurements on individual cable bacteria filaments that allow us to quantify a voltage drop along cable bacteria filaments and show a transport of electrons over several mm. This is orders of magnitude longer than previously known for biological electron transport. \body

Main text:

Cable bacteria are multicellular, centimeter-long filamentous bacteria that occur globally in marine and freshwater sediments (1–5). In their presence the sediment exhibits an electrical coupling between the oxidation of sulfide (H_2S) in deeper sediment layers and the reduction of oxygen (O_2) near the sediment-water interface, thereby generating a 1-4 cm deep suboxic zone devoid of O_2 and H_2S (6, 7). Cable bacteria spanning this suboxic zone thus appear to transfer electrons over centimeter distances, which is several orders of magnitude longer than previously found in any organism (1, 7–10). Long-distance electron transport by cable bacteria is supported by several observations: (i) changes in oxygen availability in the water

column have an immediate effect on sulfide oxidation several centimeters into the sediment, which is faster than what can be explained by diffusion (6); (ii) electron transport occurs even where cable bacteria span a non-conductive barrier in the sediment like an inserted glass bead layer or a filter with pore size ≥ 2 μm (1); and (iii) a wire cutting through the suboxic zone rapidly disrupts conduction (1). However, direct demonstration of electric conductance by individual cable bacteria filaments is still lacking (1, 11).

The mechanism of conductance has remained unclear but continuous periplasmic fibers, running along the entire filament length, have been proposed as conducting elements (1). Electrostatic force microscopy measurements indicated a significant charge storage capacity in these fibers (1). Capacitance has also been observed in another electrogenic bacterium, *Geobacter sulfurreducens*, where it is due to abundant c-type cytochromes (12). The type and redox state of cytochromes can be analyzed using resonance Raman microscopy (13), and this method has revealed gradients in cytochrome redox states in electrically conductive *Geobacter* biofilms (14–16). We hypothesized that any electron conduction by the cable bacteria from sulfide to oxygen must be associated with a potential gradient along the conductive structure (7). Since cytochromes are common electron carriers in bacterial cells, we further hypothesized that, as seen in *Geobacter* biofilms, this potential gradient should be reflected by the redox state of cytochromes. Here we used resonance Raman microscopy as a noninvasive technique to detect a gradient in cytochrome redox state along living cable bacteria filaments and to demonstrate its dependence on an intact electrical connection between the electron donor H_2S and the electron acceptor O_2.

Results

Positioning of living cable bacteria in gradients of sulfide and oxygen

We constructed a microscope chamber setup (Fig. S1) that allowed to position individual cable bacterium filaments between a sulfide source and an oxygen source located 5 mm apart from each other (17) (see Supplementary Materials for details). Sediments from one freshwater site and two marine sites were enriched for cable bacteria (see Supplementary Materials) and used as source of sulfide and cable bacteria. Within a day, cable bacteria emerged from the sediment and reached the oxic zone near the air inlet (see Movie S1 and (17)). Cable bacteria filaments, which had emerged from the sulfidic sediment but had not yet reached the oxic zone were used as controls. Swarming, microaerophilic single-celled

bacteria positioned themselves approx. 1 mm from the air inlet (Fig. 1A), and microsensor measurements showed that this bacterial veil provided a good marker for the oxic-anoxic transition zone. Microsensor measurements further confirmed the absence of sulfide and oxygen in a 4 mm wide suboxic zone between the veil and the sediment edge (Fig. 1B).

Resonance Raman microscopy reveals c-type cytochromes in cable bacteria

We recorded nearly 2,000 Raman spectra for 15 cable bacteria filaments, which spanned the suboxic zone from sulfide to oxygen. Cable bacteria diameters ranged from 1.6 to 6.6 µm, and only motile filaments were used, as these are certain to be metabolically active. All filaments displayed the four most prominent bands reported for *c*-type cytochromes at 750 (ν_{15} pyrrole breathing mode), 1130 (ν_{22}), 1315 (ν_{21}), and 1588 cm^{-1} (ν_2) (Fig. 2A, S2, S3)(17), which all decreased in intensity across the suboxic zone from near the sediment to the oxygen front. Thick filaments (> 4 µm diameter) provided more detailed spectra, with additional small bands of several vibrational modes of the cytochrome heme groups (Fig. 2A, S2). Near the sediment, the ν_4 and ν_3 bands were centered at 1361 and 1496 cm^{-1}, respectively (Fig. 2A and S2, red trace). Near the oxic zone, the overall spectra intensity decreased, the ν_4 band shifted to 1369 cm^{-1}, the ν_3 band was no longer detectable, and a broad ν_{10} mode at 1637 cm^{-1} appeared (Fig. 2A, B, and S2, blue trace). All these changes are consistent with a *c*-type heme having a six-coordinated low-spin central iron atom varying its oxidation state from reduced (near the sediment) to oxidized (near oxygen)(18, 19). Broadening of the ν_2 (featuring a shoulder at 1593 cm^{-1}) and ν_{10} bands suggests the presence of at least two different conformers having His-Fe-His and His-Fe-Met axial ligation (18). Both of these conformers were also detected for *Geobacter* species grown on electrodes, where these cytochromes connect the cell metabolism to the electrode (13, 20).

Cytochrome redox state changes gradually along the cable bacterium filaments

Throughout the rest of the study, the most prominent band in all cable bacteria filaments, at 750 cm^{-1} (Fig. 2A, S3), was used as proxy of cytochrome redox state (21, 22). Along all cable bacterium filaments connected to both O_2 and H_2S (N=15), we observed a gradual decrease of the absolute intensity of this 750 cm^{-1} band from the sulfidic sediment towards the oxic zone (Fig. 2B, C, S4). In the subset of thick filaments (N=6), we also observed a gradual

increase of the band at 1637 cm^{-1}. In contrast, filaments without connection to oxygen (N = 3) showed highly reduced spectra (N = 300) with high intensities of the 750 cm^{-1} band, even close to the oxic-anoxic transition. Filaments briefly incubated in oxic water (N = 4) all showed spectra typical for oxidized cytochromes (N = 98), with low intensities at 750 cm^{-1} (Fig. S5). These controls demonstrate that the observed differences in cytochrome band intensities along cable bacteria filaments were not due to varying cytochrome abundance along the filaments, but are caused by the cytochrome redox state.

Fast shift in cytochrome redox state upon disconnection of O_2

In order to directly link the change in cytochrome redox state to electron transport along individual bacterial cables, we used two experimental manipulations that have previously been demonstrated to impede the electron flow in sediment cores with cable bacteria activity (1, 6).

First, we removed oxygen from the air inlet by either filling the inlet with oxygen-free water or by flushing it with dinitrogen gas (Fig. 3A). Within approx. 10 min, the cytochrome redox state near the sediment, i.e. 4 mm away from the site of manipulation, showed a small but significant shift towards a more reduced pattern (Fig. 3B). This shift was more pronounced at the center of the suboxic zone (midpoint; Fig. 3A-B), where the initial cytochrome redox state was more oxidized, in concordance with the redox potential gradient from sediment to oxic zone (Fig. 2C). The shift could be reversed by reintroducing oxygen, which re-established the original redox state within 3 min, i.e., as fast as we could measure (Fig. 3C). Cable bacteria filaments connected to the sediment but not to the oxic zone (Fig. 3A) had already highly reduced cytochromes and showed no change upon removal of oxygen.

In a second experiment, we stopped the electron transport by cutting individual filaments using a laser microdissection microscope and measured the response in cytochrome redox state near the sediment edge (Fig 4A). An advantage of this approach is that cutting a single filament will have only limited effects on sulfide and oxygen gradients. Within 5 minutes, a clear shift towards more reduced cytochromes was detected in the part of the cable filament that was still connected to the sediment (Fig. 4B). Cable bacteria not reaching the oxic zone showed no change in cytochrome redox state upon cutting.

Discussion

In both manipulation experiments, we observed a significant shift towards more reduced cytochromes when filaments were no longer connected to oxygen. With the terminal electron acceptor suddenly unavailable, cytochromes in the cable bacteria apparently accumulate electrons released by sulfide oxidation in the sediment and thereby become more reduced. The response time of minutes is too fast to be explained by diffusion of chemical compounds over a distance of millimeters either outside or inside the cable bacteria filaments. Therefore, we infer from our manipulation experiments that the rapid changes observed in the cytochrome redox state must depend on the capability of transporting electrons across millimeter distances from the sulfidic zone to the oxic zone.

At present, the exact role of the cytochromes in cable bacteria-mediated electron transport from electron donor to electron acceptor remains elusive. The gradual change in cytochrome redox state cannot result from a change in the external redox conditions, as both oxygen and sulfide were absent from the intermediate, suboxic zone. The redox state of the cytochromes thus reflects an internal redox potential gradient within individual cable bacteria filaments, which is consistent with three scenarios. First, the cytochromes could theoretically be part of the conductive structure, which would then suggest a mechanism of electron-hopping via heme groups along the redox gradient (14, 23). However, the electron hopping frequency and the amount of heme groups required to explain the observed rates of electron transport would be unprecedented (7). Secondly, cytochromes could operate in combination with pilus nanowires, as proposed for electroactive biofilms thicker than 10 µm (24). Finally, the cytochromes could be involved in the up- and downloading of electrons to and from a yet unknown internal conductive structure (Fig 1D). Analogous to how a voltmeter measures the electrical potential gradient along the length of a resistor, the cytochromes would then measure the potential gradient along the conductor. The observed gradient in cytochrome redox states thus reflects the voltage drop along the internal conductor of the cable bacteria.

This voltage drop can be quantified applying the Nernst equation and the ratio of reduced to oxidized cytochromes at either side of the suboxic zone (for details see SI Material and Methods). Using the cable bacteria filaments with the largest diameters and thus the best-quality Raman spectra (Fig. S4I-O), we calculated a voltage drop of 12.3-14.6 ± 3.8-4.1 mV mm^{-1} (mean ± SD; N = 6; Table S1). This voltage drop represents energy loss in the conductor. If extrapolated to the natural setting, where cable bacteria typically span suboxic

zones of 20 mm, the voltage drop would be up to 293 mV to maintain the same current. Considering the theoretical maximum of about 1000 mV available for aerobic sulfide oxidation, this is a significant dissipation of energy and it is suggested that extension of the operational length of a cable bacterium eventually forces a lower current or a lower energy yield per electron transferred.

These findings hence provide the first direct evidence of long-distance electron conduction in individual cable bacteria, which in our experiments takes place over several mm, i.e. about 1000x the length of individual cells. In natural sediments, long-distance electron transport by cable bacteria is extended to centimeter distances (6).

Methods

Please see SI Appendix for a detailed description of the materials and methods.

Sampling and incubation

Surface sediment was collected from a freshwater lake and two marine sites containing cable bacteria of the genera *Candidatus* Electronema and *Ca*. Electrothrix (4). The sediments were enriched in the laboratory for cable bacteria as previously described (1) and used for transfer to microscope chamber setups.

Microscope chamber setups

Two microscope chamber setups (A and B, Fig. S1) were used to examine cable bacteria filaments. Both setups mimicked the redox gradient conditions that cable bacteria experience in their natural habitat, with a sulfide source (sediment) on one side, and an oxygen source (air) on the other side. In setup A, two wells (diameter 1-4 mm, separation 5 mm) were drilled into 4 mm-thick glass microscopy slides using a diamond drill. One well was filled with the cable bacteria-enriched sediment, while the other was left open and hence filled with ambient air. Cable bacteria reached out of the sediment and moved across the water zone towards the air-filled well within 24 hours (Movie S1).

In setup B, glass slabs were glued onto a microscope slide, creating a trench in the middle, which was filled with the cable bacteria-enriched sediment and covered with a cover slip. As in setup A, cable bacteria reached out of the sediment towards the oxic zone near the edge of the microscope slide.

Oxygen and hydrogen sulfide microsensor measurements

Microelectrodes for O_2 and H_2S were inserted between the microscope slide and the cover slip of slide setup B. O_2 and H_2S concentration were recorded from the edge of the cover slip until 2 mm into the suboxic zone, or all the way into the sediment, respectively.

Resonance Raman microscopy

Raman spectra were recorded on confocal Raman microscopes (Horiba and Renishaw) along individual filaments of cable bacteria starting from the sediment and moving towards the air-inlet. At each longitudinal position, 2-3 line scans with 10-20 measuring points each were performed across the filament. The ν_{15} (at 750 cm^{-1}) and the ν_{10} vibrational modes (at 1637 cm^{-1}) were used as measure of cytochrome redox state, and data reported for each filament position are means of the quality-filtered and normalized band intensities (see 'Data Analysis' in SI Material and Methods). Statistical analyses are described in SI Material and Methods.

Manipulation experiments

Two manipulation experiments were performed where electron transport was inhibited and the change in cytochrome redox state was recorded by Raman microscopy. First, oxygen was removed from the oxic end of slide setup A by either filling the air inlet with nitrogen-flushed, oxygen-free water or by flushing it directly with a gentle flow of nitrogen gas. Raman spectra were recorded at approx. 500 µm from the sediment and at the midpoint between the sediment and the start of the oxic zone every 1-3 min over a period of 15-30 min before and after the manipulation. The first 5 min after removing oxygen were excluded to account for the time it took to fully deplete oxygen at the end of the cable bacteria. Oxygen was re-introduced by stopping the flow of nitrogen gas, and the response in cytochrome redox state was immediately recorded at midpoint only. Second, a laser microdissection microscope (Leica, Germany) was used to make two cuts 10 µm apart in the cable bacteria filament, approx. 1000 µm from the sediment. Raman spectra were recorded at approx. 500 µm from the sediment, directly before and about 5 min after the cut. In both experiments, the band intensity at 750 cm^{-1} before the manipulation was normalized to 1, and any response to the manipulation is given as fold-change relative to that value. Cable bacteria filaments, which were only connected to the sediment but did not reach the oxic zone, were used as controls.

Acknowledgements:

We thank Lars B. Pedersen and Preben G. Sørensen for help with making the customized micro-sensors, Simon Agner Holm for providing the movie of cable bacteria, Anton Tramper, Silvia Hidalgo-Martinez, and Diana Vasquez-Cardenas for sediment collection, incubation and transport, and Arno Schintlmeister and Bo Barker Jørgensen for valuable discussions. This study was supported by the European Research Council (Advanced Grant: Coulombus 291650), the Danish National Research Foundation (DNRF104 and DNRF136), and The Danish Council for Independent Research | Natural Sciences (FNU) and Technology and Production Sciences (FTP). DB was supported in part by Austrian Science Fund (P26127-B20 and P27831-B28) and European Research Council (Starting Grant: FunKeyGut 741623). DM acknowledges the Netherlands Organisation for Scientific Research (NWO) grant 722.011.003. PT was supported by the European Research Council under the European Union's Seventh Framework Program (FP7/20072013, European Research Council grant 311341). FJRM was supported by the European Research Council (Grant: SedBioGeoChem 306933), the Research Foundation Flanders (FWO grant G031416N) and VICI grant 016.VICI.170.072 from NWO. MW was supported by the European Research Council (Advanced Grant: NITRICARE 294343).

1. Pfeffer C, et al. (2012) Filamentous bacteria transport electrons over centimetre distances. *Nature* 491(V):10–13.

2. Malkin SY, et al. (2014) Natural occurrence of microbial sulphur oxidation by long-range electron transport in the seafloor. *ISME J* 8(9):1843–1854.

3. Risgaard-Petersen N, et al. (2015) Cable bacteria in freshwater sediments. *Appl Environ Microbiol* 81(17):6003–6011.

4. Trojan D, et al. (2016) A taxonomic framework for cable bacteria and proposal of the candidate genera Electrothrix and Electronema. *Syst Appl Microbiol* 39(5):297–306.

5. Burdorf LDW, et al. (2017) Long-distance electron transport occurs globally in marine sediments. *Biogeosciences* 14(3):683–701.

6. Nielsen LP, Risgaard-Petersen N, Fossing H, Christensen PB, Sayama M (2010) Electric currents couple spatially separated biogeochemical processes in marine sediment. *Nature* 463(7284):1071–4.

7. Meysman FJR, Risgaard-Petersen N, Malkin SY, Nielsen LP (2015) The geochemical fingerprint of microbial long-distance electron transport in the seafloor. *Geochim Cosmochim Acta* 152:122–142.

8. Lovley DR (2017) Syntrophy goes electric: direct interspecies electron transfer. *Annu Rev Microbiol* 71(1):644–657.

9. Schauer R, et al. (2014) Succession of cable bacteria and electric currents in marine sediment. *ISME J* 8(6):1314–22.

10. Risgaard-Petersen N, Revil A, Meister P, Nielsen LP (2012) Sulfur, iron-, and calcium cycling associated with natural electric currents running through marine sediment. *Geochim Cosmochim Acta* 92:1–13.

11. Meysman FJR (2017) Cable bacteria take a new breath using long-distance electricity. *Trends Microbiol*:1–12.

12. Esteve-Núñez A, Sosnik J, Visconti P, Lovley DR (2008) Fluorescent properties of c-type cytochromes reveal their potential role as an extracytoplasmic electron sink in Geobacter sulfurreducens. *Environ Microbiol* 10(2):497–505.

13. Virdis B, Harnisch F, Batstone DJ, Rabaey K, Donose BC (2012) Non-invasive characterization of electrochemically active microbial biofilms using confocal Raman microscopy. *Energy Environ Sci* 5(5):7017.

14. Lebedev N, Strycharz-Glaven SM, Tender LM (2014) Spatially resolved confocal resonant Raman microscopic analysis of anode-grown Geobacter sulfurreducens biofilms. *ChemPhysChem* 15(2):320–327.

15. Robuschi L, Tomba JP, Busalmen JP (2017) Proving Geobacter biofilm connectivity with confocal Raman microscopy. *J Electroanal Chem* 793:99–103.

16. Snider RM, Strycharz-Glaven SM, Tsoi SD, Erickson JS, Tender LM (2012) Long-range electron transport in Geobacter sulfurreducens biofilms is redox gradient-driven. *Proc Natl Acad Sci* 109(38):15467–15472.

17. Bjerg JT, Damgaard LR, Holm SA, Schramm A, Nielsen LP (2016) Motility of electric cable bacteria. *Appl Environ Microbiol* 82(13):3816–3821.

18. Oellerich S, Wackerbarth H, Hildebrandt P (2002) Spectroscopic characterisation of

nonnative conformational states of cytochrome c. *JPhysChemB* 106:6566–6580.

19. Kranich A, Ly HK, Hildebrandt P, Murgida DH (2008) Direct observation of the gating step in protein electron transfer: electric-field-controlled protein dynamics. *J Am Chem Soc* 130:9844–9848.

20. Robuschi L, et al. (2013) Spectroscopic slicing to reveal internal redox gradients in electricity-producing biofilms. *Angew Chemie - Int Ed* 52(3):925–928.

21. Brazhe NA, et al. (2012) Mapping of redox state of mitochondrial cytochromes in live cardiomyocytes using raman microspectroscopy. *PLoS One* 7(9):1–8.

22. Adar F (1978) Resonance Raman spectra of ferric cytochrome c. A probe of low-lying electronic levels of the iron ion. *J Phys Chem* 82(2):230–234.

23. Strycharz-Glaven SM, Snider RM, Guiseppi-Elie A, Tender LM (2011) On the electrical conductivity of microbial nanowires and biofilms. *Energy Environ Sci* 4(11):4366.

24. Steidl RJ, Lampa-Pastirk S, Reguera G (2016) Mechanistic stratification in electroactive biofilms of Geobacter sulfurreducens mediated by pilus nanowires. *Nat Commun* 7(12217). doi:10.1038/ncomms12217.

Figure Legends

Figure 1.

(A) Dark field micrograph of cable bacteria in the microscopic chamber setup reaching from sulfidic sediment (left) to oxygen (right). Arrows show the position of the veil composed of swarming microaerophilic microbes (white) and the positions, where the reduced (red) and oxidized (blue) Raman spectra shown in Fig. 2A were recorded. (B) Sulfide (red) and oxygen (blue) concentration gradients across the chamber setup as determined by microsensor measurements (N = 6). Grey shading indicates the microaerophilic veil.

Figure 2

(A) Raman spectra from an individual cable bacterium filament (site Rattekai, NL) near sediment (red) and near oxygen (blue). (B) Difference in normalized band intensity between either ends of the suboxic zone. Red = data points closest to sediment (Figures 1F and S4); blue = data points closest to microaerophilic veil and oxygen. Stippled and open bars display band intensities at 750 and 1637 cm^{-1}, respectively, given as percentage of the maximum band intensities (mean ± standard deviation). Asterisks depict significant differences between cable bacteria ends. N (for 750 cm^{-1}/1637 cm^{-1} band) = 15/6 filaments (379/200 spectra, Shapiro-Wilk test p-value: 0.493/0.28, t-test p-value = $5.31*10^{-6}$/ $8.8*10^{-4}$). (C) Normalized band intensities (mean ± standard deviation) showing the cytochrome redox gradient along a single cable bacterium filament (Fig. S4M), reaching from sediment (to the left) towards oxygen. Grey shading indicates the microaerophilic veil.
(D) Conceptual model of electron transport in cable bacteria. Cells in the sulfidic zone, with reduced cytochromes, upload electrons from H_2S to periplasmic fibers, while cells in the oxic zone, with oxidized cytochromes, download electrons from these fibers to O_2.

Figure 3.

Effect of oxygen availability on cable bacteria redox state. (A) Schematic of the setup for oxygen manipulation experiments. A filament (light grey wave) reaches out from sulfidic sediment (left) towards the air inlet (right), from which oxygen can be removed; dark grey shading indicates the position of the microaerophilic veil. Filaments that did not reach the veil were used as controls. Positions of Raman spectra recordings are marked with red (near sediment) and purple (midpoint) arrows. (B) Change in cytochrome redox state resulting from a change in oxygen availability. Bars represent fold change in normalized band

intensities at 750 cm^{-1} relative to the intensity in the presence of oxygen (mean ± standard deviation). Significant changes in redox state are marked by an asterisk. N = 16 filaments near sediment (1666 spectra, Shapiro-Wilk test p-value: 0.0003, Wilcoxon sign test p-value: 0.000122), N = 4 filaments at midpoint (50 spectra, Shapiro-Wilk test p-value: 0.551, t-test p-value: 0.000488), and N = 6 control filaments near sediment (744 spectra, Shapiro-Wilk test p-value: 0.903, t-test p-value: 0.659). (C) Change in cytochrome redox state (band intensity at 750 cm^{-1}) of a single cable bacterium filament over time (42 min) during changes in oxygen availability. Measurements were done at midpoint. White area represents time when the air inlet was flushed with N_2; shaded blue area represents time with oxygen available.

Figure 4.

Effect of filament cutting on cable bacteria redox state. (A) Schematic of the setup for laser cut experiments. A filament (light grey wave) reaches out from sulfidic sediment (left) towards the air inlet (right); dark gray shading indicates the position of the microaerophilic veil. Filaments that did not reach the veil were used as controls. Positions of Raman spectra recordings are marked with red arrows (near sediment), positions of laser cuts are marked with green bars. (B) Change in cytochrome redox state in response to laser cutting of the filaments. Bars represent fold change in normalized band intensities at 750 cm^{-1} relative to the intensity before the cut (mean ± standard deviation). A significant change in redox state is marked by an asterisk. N = 10 filaments (1143 spectra, Shapiro-Wilk test p-value: 0.117, t-test p-value: 0.000517) and N = 5 control filaments (852 spectra, Shapiro-Wilk test p-value: 0.84, t-test p-value: 0.879).

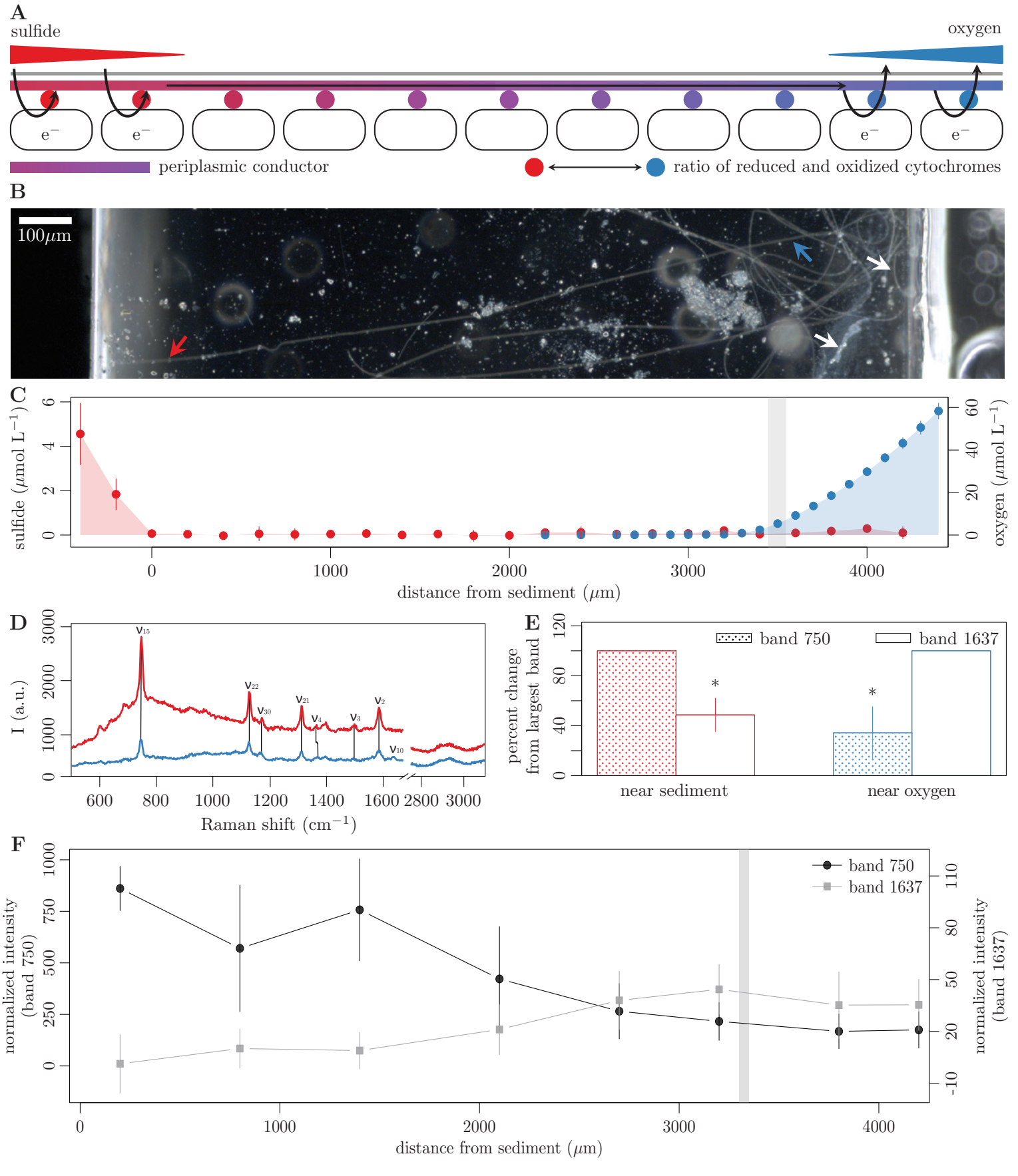
A
sulfide
oxygen
e⁻
e⁻
e⁻
e⁻
periplasmic conductor
ratio of reduced and oxidized cytochromes
B
100μm
C
sulfide (μmol L⁻¹)
oxygen (μmol L⁻¹)
distance from sediment (μm)
D
I (a.u.)
Raman shift (cm⁻¹)
E
percent change from largest band
band 750
band 1637
near sediment
near oxygen
F
normalized intensity (band 750)
normalized intensity (band 1637)
band 750
band 1637
distance from sediment (μm)

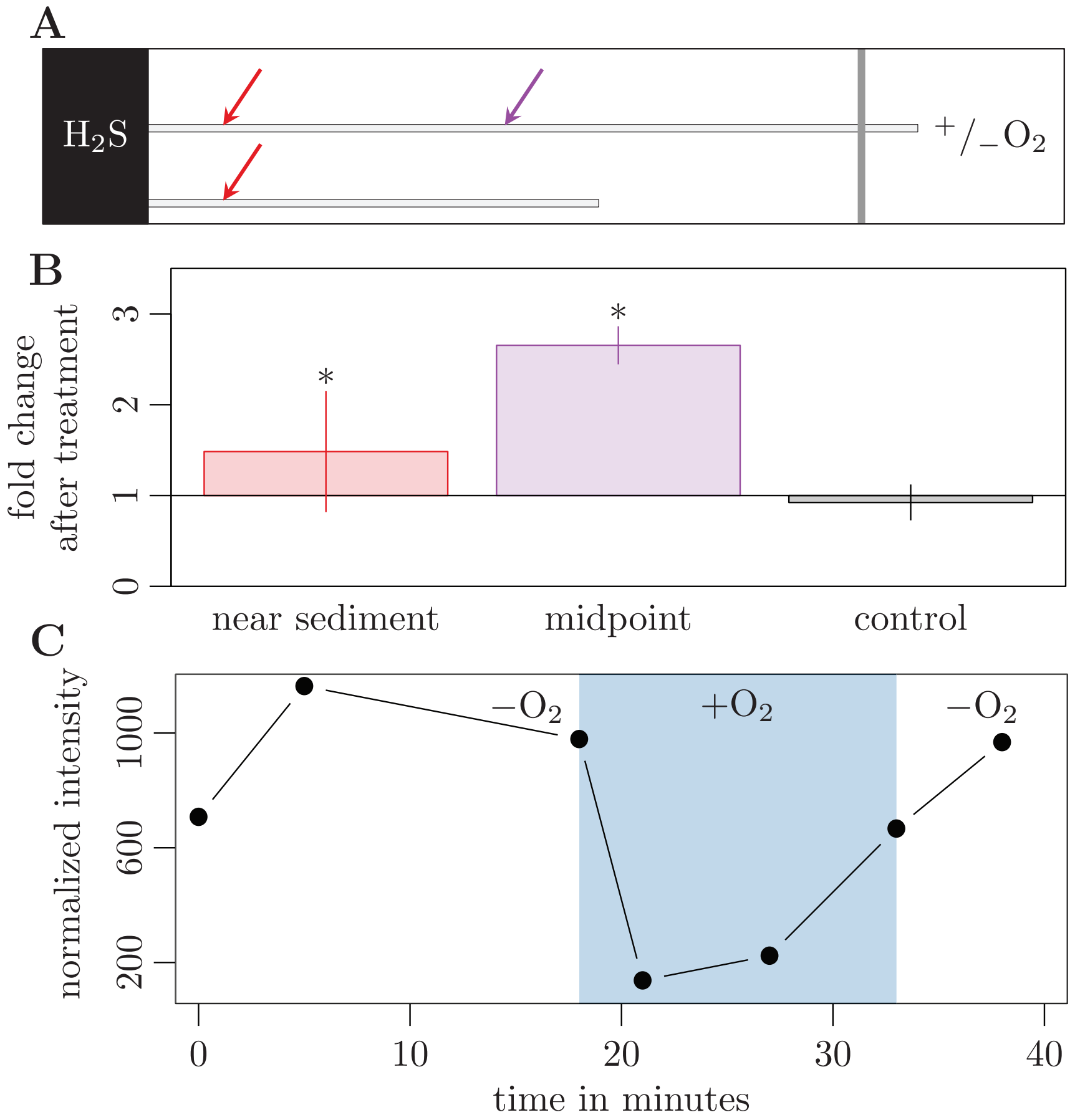
A
H_2S
+/−O_2
B
fold change after treatment
0
1
2
3
*
*
near sediment
midpoint
control
C
normalized intensity
200
600
1000
$-O_2$
$+O_2$
$-O_2$
0
10
20
30
40
time in minutes

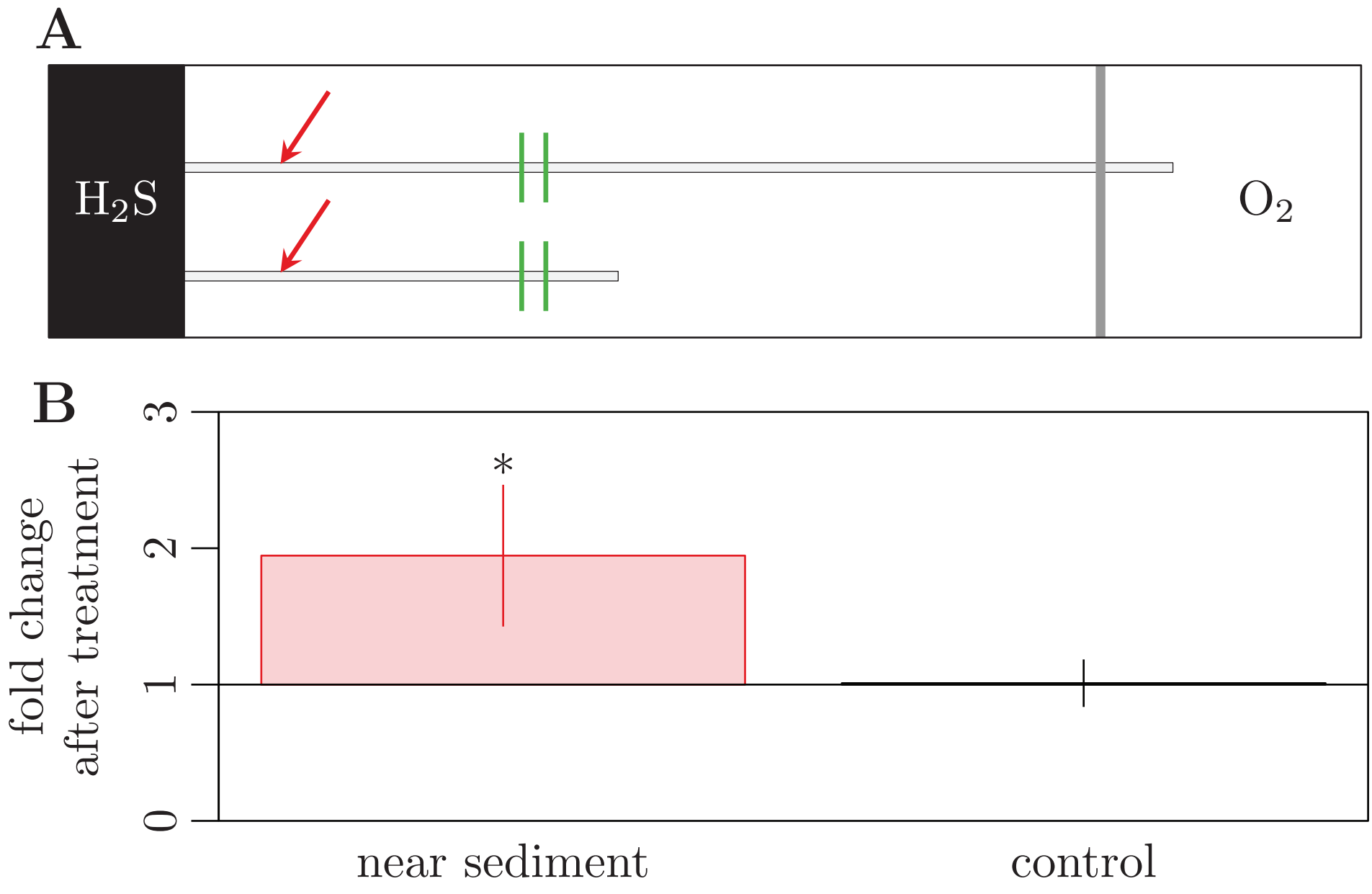
A
H_2S
O_2
B
fold change
after treatment
0
1
2
3
*
near sediment
control

Supporting Information Appendix

Jesper T. Bjerg, Henricus T.S. Boschker, Steffen Larsen, David Berry, Markus Schmid, Diego Millo, Paula Tataru, Filip J. R. Meysman, Michael Wagner, Lars Peter Nielsen, and Andreas Schramm. Long distance electron transport in individual cable bacteria.

Detailed Materials and Methods

Sampling and incubation

Surface sediment was collected from three locations containing cable bacteria of the genera *Candidatus* Electronema and *Ca*. Electrothrix (1): a freshwater lake at Aarhus University Campus, Denmark (56°16'47''N, 10°20'79''E), a marine salt marsh at Rattekaai, The Netherlands (51°26'21''N, 04°10'11''E), and an intertidal mud flat at Mokbaai, Texel, The Netherlands (53°00'27.1''N, 4°45'05.1''E). Sediments were sieved, homogenized, and incubated at 15°C with either oxygenated overlying water or an air-exposed sediment surface. The development of cable bacteria was monitored by microscopy and their metabolic activity evaluated by O_2, H_2S and pH microsensor measurements (2, 3) as previously described (4). When the sediment showed a clear geochemical fingerprint of electrogenic sulfur oxidation (as determined by O_2, H_2S and pH microsensor profiling) and revealed abundant cable bacteria (as detected by microscopy), sediments were used for transfer to the microscope chamber setups.

Microscope chamber setups

Two microscope chamber setups (A and B, Fig. S1) were used to examine cable bacteria filaments. Both setups mimicked the redox gradient conditions that cable bacteria experience in their natural habitat, with a sulfide source (sediment) on one side, and an oxygen source (air) on the other side. In setup A, two wells (diameter 1-4 mm, separation 5 mm) were drilled into 4 mm-thick glass microscopy slides using a diamond drill. One well was filled with the cable bacteria-enriched sediment, while the other was left open and hence filled with ambient air. Tap water or seawater (depending on the sediment source) was flushed with nitrogen gas and pipetted onto the microscope slide in between the two wells, the wells and interspace were covered by a coverslip (25 x 40 mm), and sealed with Vaseline or silicon grease to prevent evaporation, thus forming a 5 mm wide, 50-100 µm high water layer between sediment and air. Cable bacteria reached out of the sediment and moved across the water zone towards the air-filled well within 24 hours (Movie S1).

In setup B, glass slabs (obtained by cutting of microscope slides) were glued onto a microscope slide, thus creating a trench (10 x 50 mm) in the middle. This trench was filled with the cable bacteria-enriched sediment, a large cover slip was mounted on top, and the slide was flooded with nitrogen gas-flushed water, creating a 5 x 50 mm water-filled interspace between the sediment trench and the edge of the cover slip. The edges of the cover slip were subsequently sealed with nail polish to prevent evaporation but allow oxygen diffusion. As in setup A, cable bacteria reached out of the sediment towards the oxic zone near the edge of the cover slip.

Oxygen and hydrogen sulfide microsensor measurements

Extra-long and thin microelectrodes for O_2 and H_2S were custom-made at Aarhus University, with a tip diameter of less than 50 µm. Microelectrodes were mounted sideways on a motorized micromanipulator, and inserted between the microscope slide and the cover slip of slide setup B. The oxygen concentration was recorded at 100 µm-step resolution, from the edge of the cover slip until the sensor was 2 mm beyond the veil of microaerophilic bacteria. For H_2S, a concentration profile was recorded from the edge of the cover slip all the way into the sediment at 200 µm-step resolution.

Resonance Raman microscopy

Most Raman spectra were recorded on a LabRAM HR Evolution confocal Raman microscope (Horiba, Germany) equipped with a 500 mW 532 nm laser, an Andor EM CCD detector adapted to 500-650 nm emissions, 300 grating with a spectral resolution of 2.8 cm^{-1}, and the pinhole set to 250 µm. Additional spectra were recorded on a Renishaw InVia confocal Raman microscope (Wotton-under-Edge, United Kingdom) equipped with a Leica light microscope with 50X air objective and 532 nm laser. The output of the laser was set between 4 and 10% of maximum power. Raman spectra were recorded along individual filaments of cable bacteria starting from the sediment and moving towards the air-inlet. At each longitudinal position, 2-3 line scans with 10-20 measuring points each were performed across the filament (i.e. perpendicular to its longitudinal axis), with 2.5-20 s exposure time for each measuring point. The ν_{15} (at 750 cm^{-1}) and the ν_{10} vibrational modes (at 1637 cm^{-1}) were used as measure of cytochrome redox state, and data reported for each filament position are means of the quality-filtered and normalized band intensities (see 'Data Analysis' below) at 750 cm^{-1} and at 1637 cm^{-1} from multiple line scans (see 'Data Analysis' below).

Manipulation experiments

Two manipulation experiments were performed where electron transport was inhibited and the change in cytochrome redox state was recorded by Raman microscopy. First, oxygen was removed from the oxic end of slide setup A by either filling the air inlet with nitrogen-flushed, oxygen-free water or by flushing it directly with a gentle flow of nitrogen gas. Raman spectra were recorded at approx. 500 µm from the sediment and at the midpoint between the sediment and the start of the oxic zone (as marked by a veil of putative microaerophilic bacteria) every 1-3 min over a period of 15-30 min before and after the manipulation. The first 5 min after removing oxygen were excluded to account for the time it took to fully deplete oxygen at the end of the cable bacteria. Oxygen was re-introduced by stopping the flow of nitrogen gas, and the response in cytochrome redox state was immediately recorded at midpoint only.

Second, a laser microdissection microscope, LMD7000 (Leica, Germany) was used to make two cuts 10 µm apart in the cable bacteria filament, approx. 1000 µm from the sediment. The cut was microscopically inspected to confirm that the filament sections had separated. Raman spectra were recorded at approx. 500 µm from the sediment, directly before and about 5 min after the cut (the time it took to move the chamber between laser microdissection and Raman microscope).

In both experiments, cable bacteria filaments, which were only connected to the sediment but did not reach the oxic zone, were used as controls.

Data analysis

Pre-processing. Raman spectra were preprocessed (5) by background correction with a sensitive non-linear iterative peak-clipping algorithm with optimized parameters (smoothing = true, iteration = 70, window = “15”).

Quality filtering. Because cable bacteria filaments are constantly moving, and measuring a cross-section takes > 1 min, it was necessary to use the C-H region of the spectra (2800 to 3000 cm^{-1}) as indicator for a cable bacterium hit. The maximum peak height between 2800 and 3000 cm^{-1} was divided by the median baseline from 2800 to 2850 cm^{-1}. All ratios from an entire filament data set were then plotted as histogram for each filament, and data sets with a bimodal distribution of ratios were discarded, as this indicated that multiple cable bacteria filaments or additional bacteria had been recorded in that data set. Of the remaining data sets, only spectra with a ratio > 3.5 were kept as “high quality spectra”, while those with a ratio < 3.5 were discarded as hits outside the cable bacteria. After the filtering, 3430 high quality

spectra remained of a total of 8729 recorded spectra.

Normalization. For the line scan measurements along cable bacteria and the two manipulation experiments, the band intensity at 750 cm^{-1} was normalized by subtracting the median of the baseline from 735 to 740 cm^{-1} and from 760 to 765 cm^{-1}, to enable comparison within an individual cable bacterium. A similar approach was used for normalization of all other bands (1130, 1315, 1497, 1588, and 1637 cm^{-1}). Means were calculated for each individual, normalized line scan, and subsequently the mean for each position or treatment was calculated from these means. Standard deviations were calculated from all individual data points for a given position.

In the two manipulation experiments, where comparison between different filaments was necessary, the band intensity at 750 cm^{-1} before the manipulation were normalized to 1, and any response to the manipulation is given as fold-change relative to that value.

Statistical Analysis

All data for which statistical analysis was performed were first tested for deviation from a normal distribution using a Shapiro-Wilk test of normality.

The normalized intensity change between the reduced and the oxidized filament ends was tested for being greater than 0 using a one-sided t-test. The observed change after oxygen and laser cutting manipulations in the normalized intensity was tested for being different than zero using a two-sided t-test (for normal data) or Wilcoxon sign test (for non-normal data). All calculations for data and statistical analysis were performed using the statistical software program R (6).

Quantifying the voltage drop along individual cable bacteria

The recorded gradients in cytochrome redox status of single filaments through the suboxic zone allow for calculation of the voltage gradient, assuming that the cytochromes are in equilibrium with the electron conductor in this zone. The local cytochrome redox potential is determined by the Nernst equation for single electron transfer:

$$\mathrm{E} = E^{0} - \frac{RT}{F} ln \frac{[Red]}{[Ox]} \qquad \text{(Equation 1)}$$

Where E^{o} is the midpotential, Red and Ox the numbers of reduced and oxidized cytochromes, and R, T, and F denote the gas constant, the absolute temperature, and the Faraday constant,

respectively. The voltage difference between two sites in the suboxic zone, near sediment (a) and near the oxic zone (b), is then

$$\mathrm{E} = E^b - E^a = \left(E^0 - \frac{RT}{F} ln \frac{[Red]^b}{[Ox]^b} \right) - \left(E^0 - \frac{RT}{F} ln \frac{[Red]^a}{[Ox]^a} \right) \qquad \text{(Equation 2)}$$

This condenses into

$$\mathrm{E} = \frac{RT}{F} ln \left(\frac{\frac{[Red]^a}{[Red]^b}}{\frac{[Ox]^a}{[Ox]^b}} \right) \qquad \text{(Equation 3)}$$

Assuming that

$$\frac{[Red]^a}{[Red]^b} = \frac{[band\,750]^a}{[band\,750]^b} \qquad \text{(Equation 4)}$$

and

$$\frac{[Ox]^a}{[Ox]^b} = \frac{[band\,1637]^a}{[band\,1637]^b} \qquad \text{(Equation 5)}$$

the voltage difference can be calculated as

$$\mathrm{E} = \frac{RT}{F} ln \left(\frac{\frac{[band\,750]^a}{[band\,750]^b}}{\frac{[band\,1637]^a}{[band\,1637]^b}} \right) \qquad \text{(Equation 6)}$$

The same equation holds when band 750 is replaced with any of the other reduction bands (1130, 1315, 1497, and 1588, cm^{-1}). Therefore, for the final calculation, we apply the ratio of all reduction bands for every filament (Table S1). For the analyzed 2.1-4.3 mm long suboxic segments of 6 large cable bacteria filaments (Rattekaai, NL), the average voltage difference, normalized to the length of the suboxic zone, was 14.6 mV mm^{-1} ± 4.1 (SD).

This result was confirmed by another measure of $[Ox]^a/[Ox]^b$ than the relatively uncertain $1637^a/1637^b$ ratio (Equation 5): The increase in band intensities near the sulfidic zone after laser-cutting (Figure 3) was assumed to represent maximum electron saturation of the

cytochromes, and thus represents the situation were all cytochromes are reduced. Therefore [Ox], being the unsaturated cytochromes, can be expressed as

$$[Ox] = [Red]^{max} - [Red] \qquad \text{(Equation 7)}$$

where $[Red]^{max}$ represents the total concentration of cytochromes.

Introducing this in Equation 4 and 5 leads to the solution

$$\frac{[Ox]^a}{[Ox]^b} = \frac{[band\,750]^{max} - [band\,750]^a}{[band\,750]^{max} - [band\,750]^b} \qquad \text{(Equation 8)}$$

As before the band 750 can be replaced with 1130, 1315, 1497, and 1588 cm^{-1} bands. For the 10 laser-cut Rattekaai cable bacteria filaments (Figure 3), the ratio Ox^a/Ox^b became 0.62 ± 0.04 SD (± 0.08 SD with Red^{max} estimate), i.e. not different from the $1637^a/ 1637^b$ ratio (0.49 ± 0.16 SD); see Table S1 for data and calculations. Using this value for the above calculation, and normalizing for length, the voltage gradients were 12.3 mV mm^{-1} ± 3.8 (SD).

***SI* Figures**

Figure S1.
(A) Microscope setup used for gradients and oxygen manipulations. Top, thick microscope slide with two wells (light gray); red bar shows the 5 mm interspace between wells. Bottom, filled slide setup with sediment in one well (dark gray), from which cable bacteria reach towards the other well (light gray, air inlet). Availability of oxygen can be manipulated at the open air inlet (marked by an arrow). (B) Microscope slide setup used for gradients and laser cuts. Top, microscope slide with long trench in the center; red bar shows the 5 mm space from trench to edge of slide. Bottom, filled slide setup with sediment (dark gray) in the trench, from which cable bacteria reach out towards the edge of the slide, where oxygen is available.

Figure S2. Raman spectra from a >4 μm thick individual cable bacterium filament from a marine salt marsh (Rattekai, NL) near sediment (red) and near oxygen (blue). An enlargement of the area between 1330 cm^{-1} and 1660 cm^{-1} of the same spectrum displayed in Figure 1D is shown.

Figure S3. (A) Raman spectra from a thin individual cable bacterium filament from freshwater sediment (Aarhus, DK) near sediment (red) and near oxygen (blue). (B) Raman spectra from an individual cable bacterium filament from intertidal mud flat (Mokbaai, Texel, NL) near sediment (red) and near oxygen (blue).

Figure S4. Cytochrome redox gradient along individual cable bacteria filaments reaching from sediment towards oxygen. The displayed values (mean ± standard deviation; N = 1-35 spectra per position) are normalized band intensities at 750 cm^{-1} (black dots) and 1637 cm^{-1} (grey squares). (A-D) Cable bacteria from freshwater sediment (Aarhus, DK). (E-H) Cable bacteria from intertidal mud flat (Mokbaai, Texel, NL). (I-O) Cable bacteria from marine salt marsh (Rattekaai, Texel, NL).

Figure S5. Cytochrome redox state (mean ± standard deviation of the normalized band 750 cm^{-1} intensities) along control cable bacteria. Red, 4 filaments in fully oxic water (98 spectra); blue, 3 filaments, which did not reach the oxic zone (301 spectra).

***SI* Material as additional files**

Movie S1. Time-lapse movie of cable bacteria emerging from sediment (left side) in the microscope chamber setup and gliding towards oxygen (to the far right). 16 min were compressed to 17 sec. Scale bar, 100 µm.

Table S1. Data and calculations to quantify the voltage drop over the length of individual cable bacteria filaments.

SI References

1. Trojan D, et al. (2016) A taxonomic framework for cable bacteria and proposal of the candidate genera Electrothrix and Electronema. *Syst Appl Microbiol* 39(5):297–306.
2. Revsbech NPN, Jørgensen BBB (1986) Microelectrodes: their use in microbial ecology. *Adv Microb Ecol* 9:293–352.
3. Jeroschewski P, Steuckart C, Kuhl M (1996) An Amperometric Microsensor for the Determination of H 2 S in Aquatic Environments. *Anal Chem* 68(24):4351–4357.
4. Pfeffer C, et al. (2012) Filamentous bacteria transport electrons over centimetre distances. *Nature* 491(V):10–13.
5. Bocklitz T, Walter A, Hartmann K, Rösch P, Popp J (2011) How to pre-process Raman spectra for reliable and stable models? *Anal Chim Acta* 704(1–2):47–56.
6. R Core team (2016) R: A Language and Environment for Statistical Computing. Available at: https://www.r-project.org/.

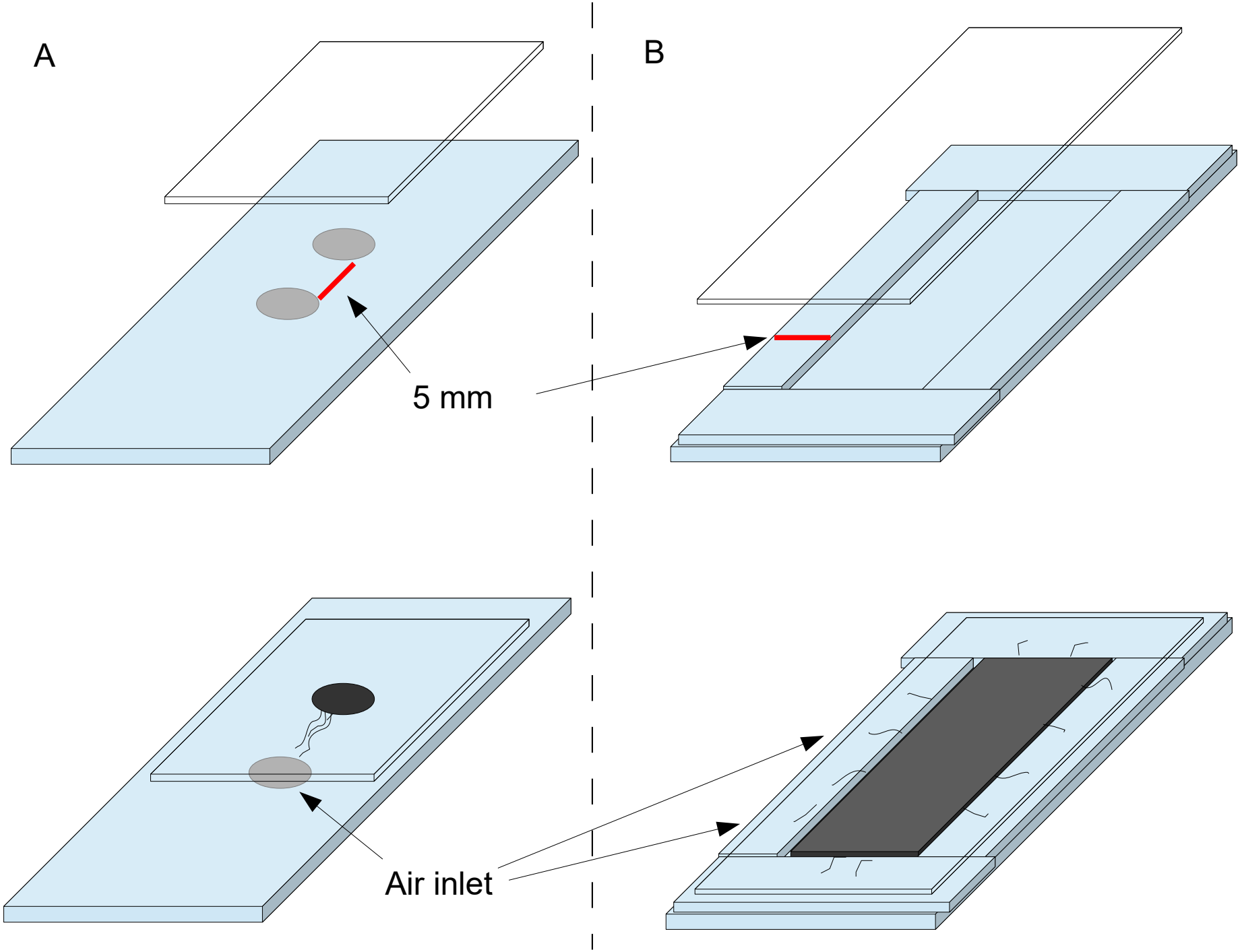
A
B
5 mm
Air inlet

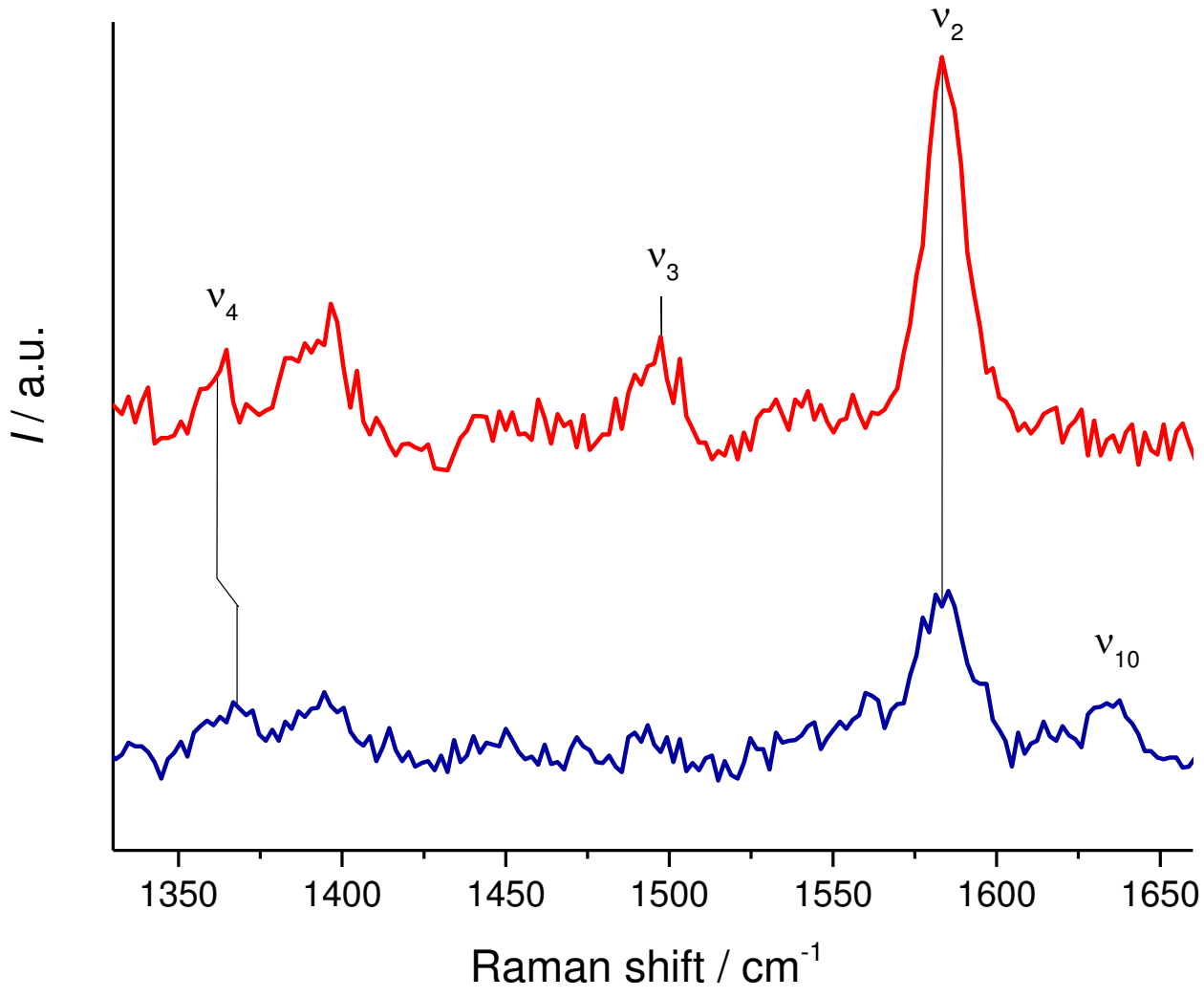
ν2
ν3
ν4
ν10
I / a.u.
1350
1400
1450
1500
1550
1600
1650
Raman shift / cm-1

A

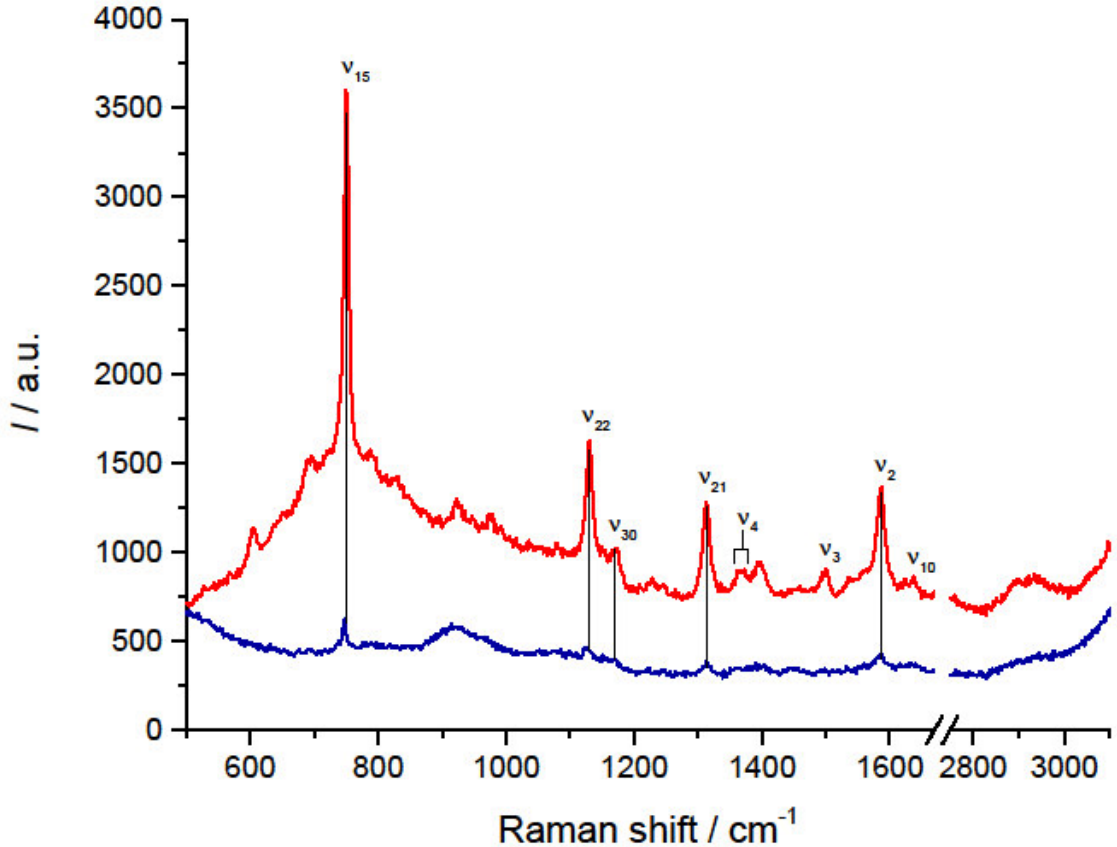
I / a.u.
Raman shift / cm-1
ν15
ν22
ν30
ν21
ν4
ν3
ν2
ν10

B

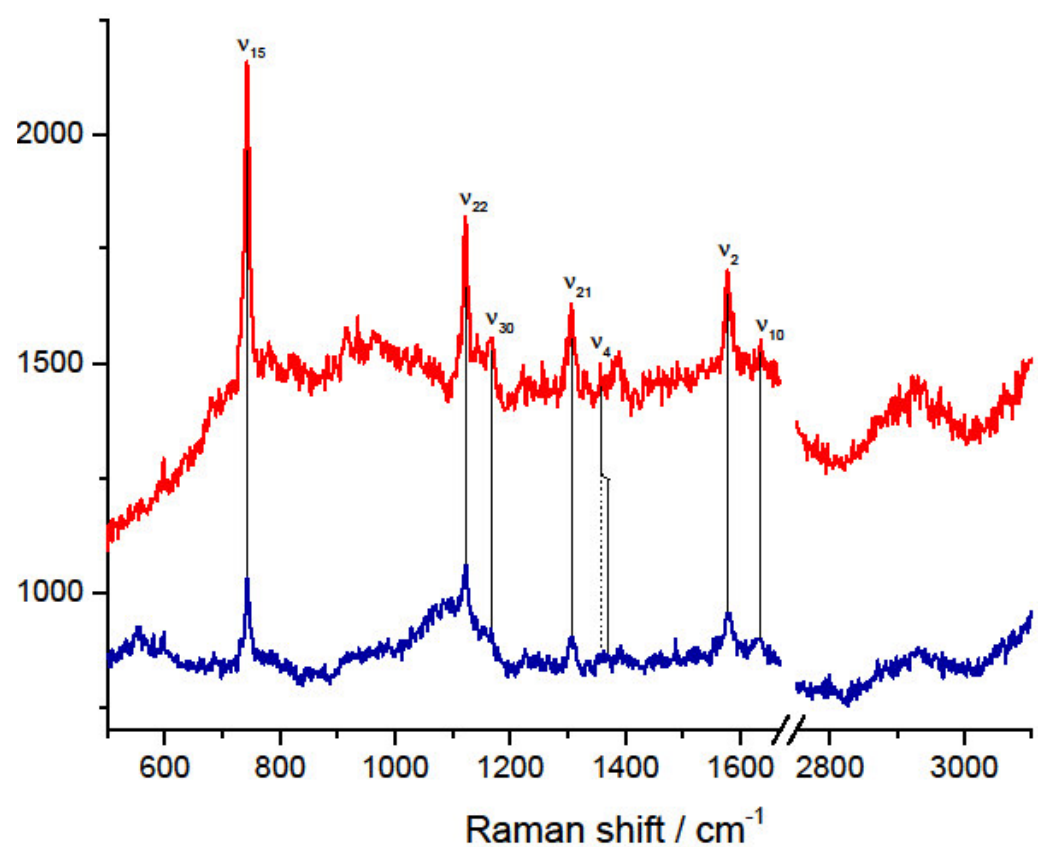
Raman shift / cm-1
ν15
ν22
ν30
ν21
ν4
ν2
ν10

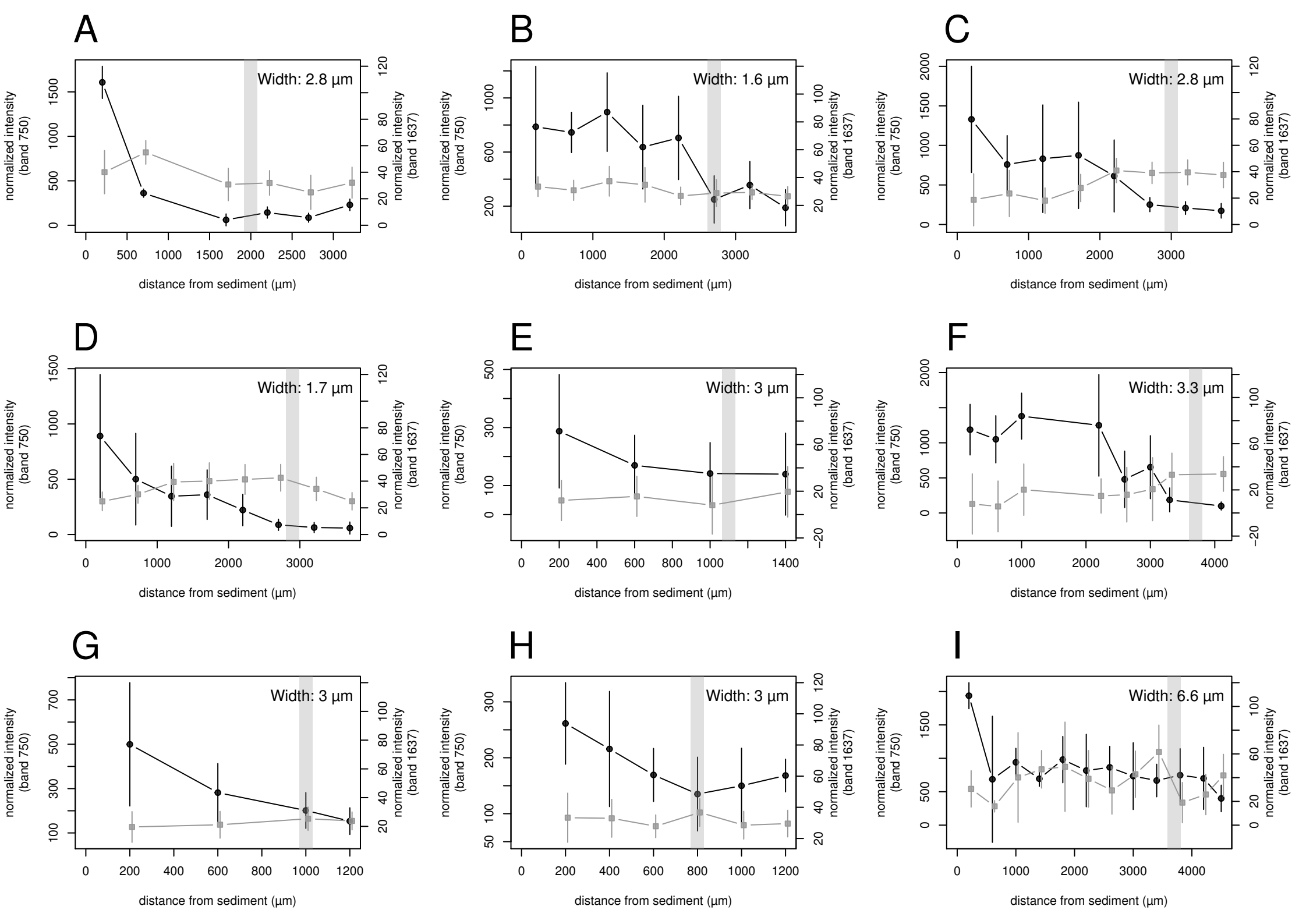
A
Width: 2.8 µm
B
Width: 1.6 µm
C
Width: 2.8 µm
D
Width: 1.7 µm
E
Width: 3 µm
F
Width: 3.3 µm
G
Width: 3 µm
H
Width: 3 µm
I
Width: 6.6 µm
normalized intensity (band 750)
normalized intensity (band 1637)
distance from sediment (µm)

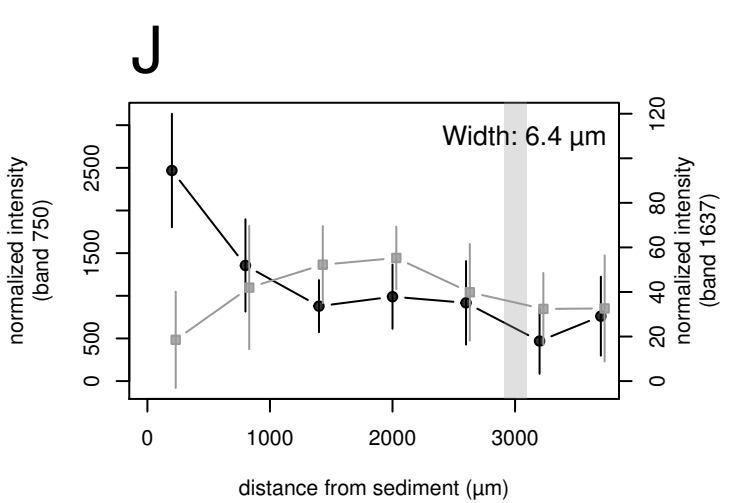
J
Width: 6.4 µm
normalized intensity (band 750)
normalized intensity (band 1637)
distance from sediment (µm)

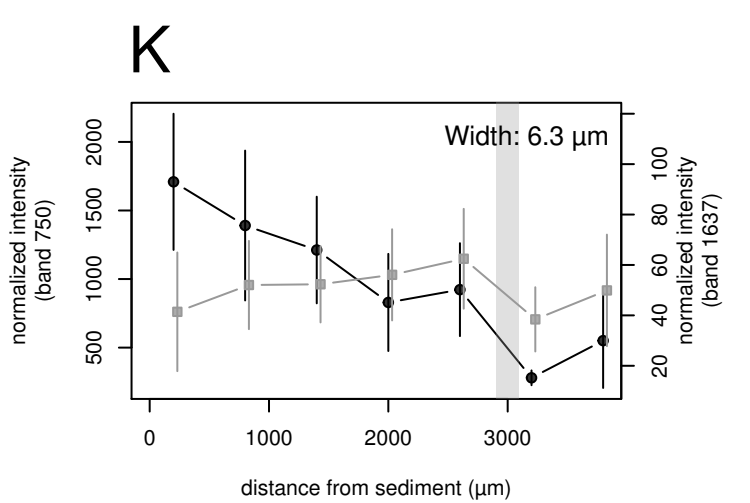
K
Width: 6.3 µm
normalized intensity (band 750)
normalized intensity (band 1637)
distance from sediment (µm)

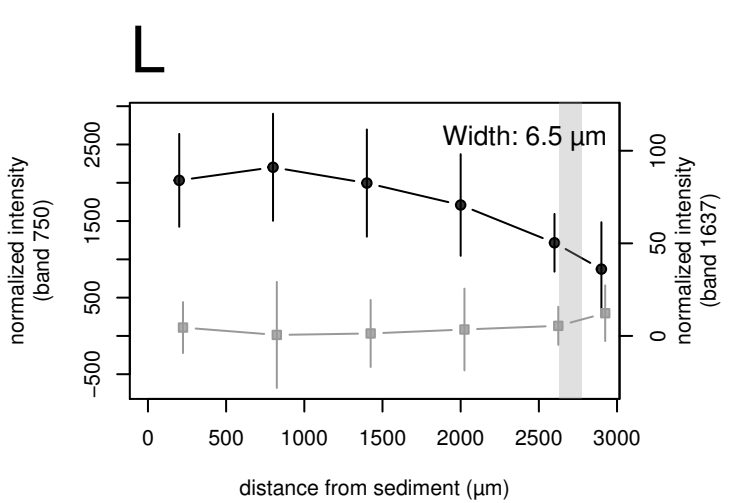
L
Width: 6.5 µm
normalized intensity (band 750)
normalized intensity (band 1637)
distance from sediment (µm)

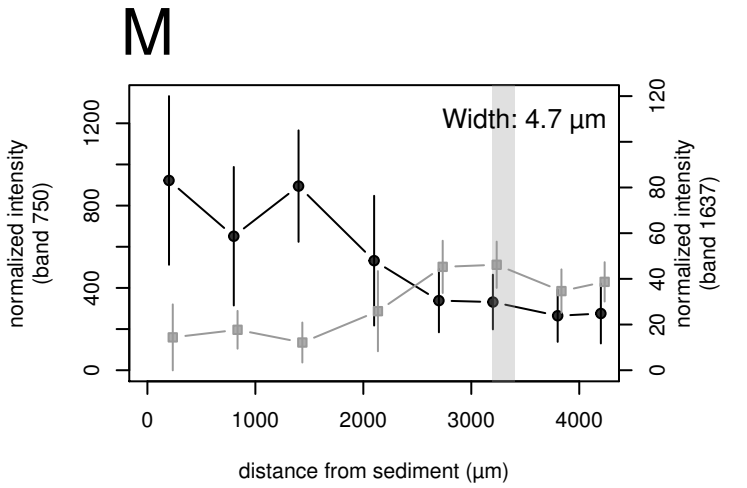
M
Width: 4.7 µm
normalized intensity (band 750)
normalized intensity (band 1637)
distance from sediment (µm)

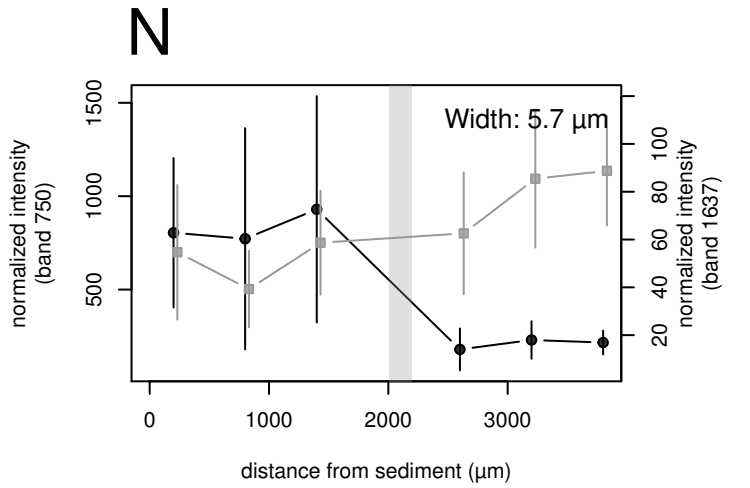
N
Width: 5.7 µm
normalized intensity (band 750)
normalized intensity (band 1637)
distance from sediment (µm)

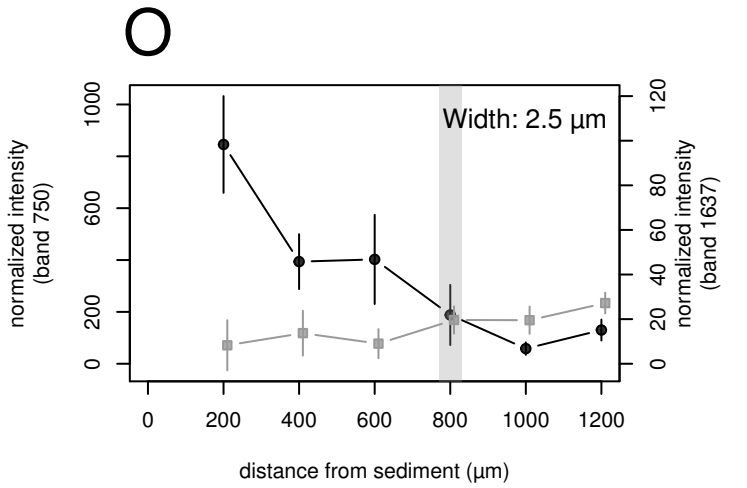
O
Width: 2.5 µm
normalized intensity (band 750)
normalized intensity (band 1637)
distance from sediment (µm)

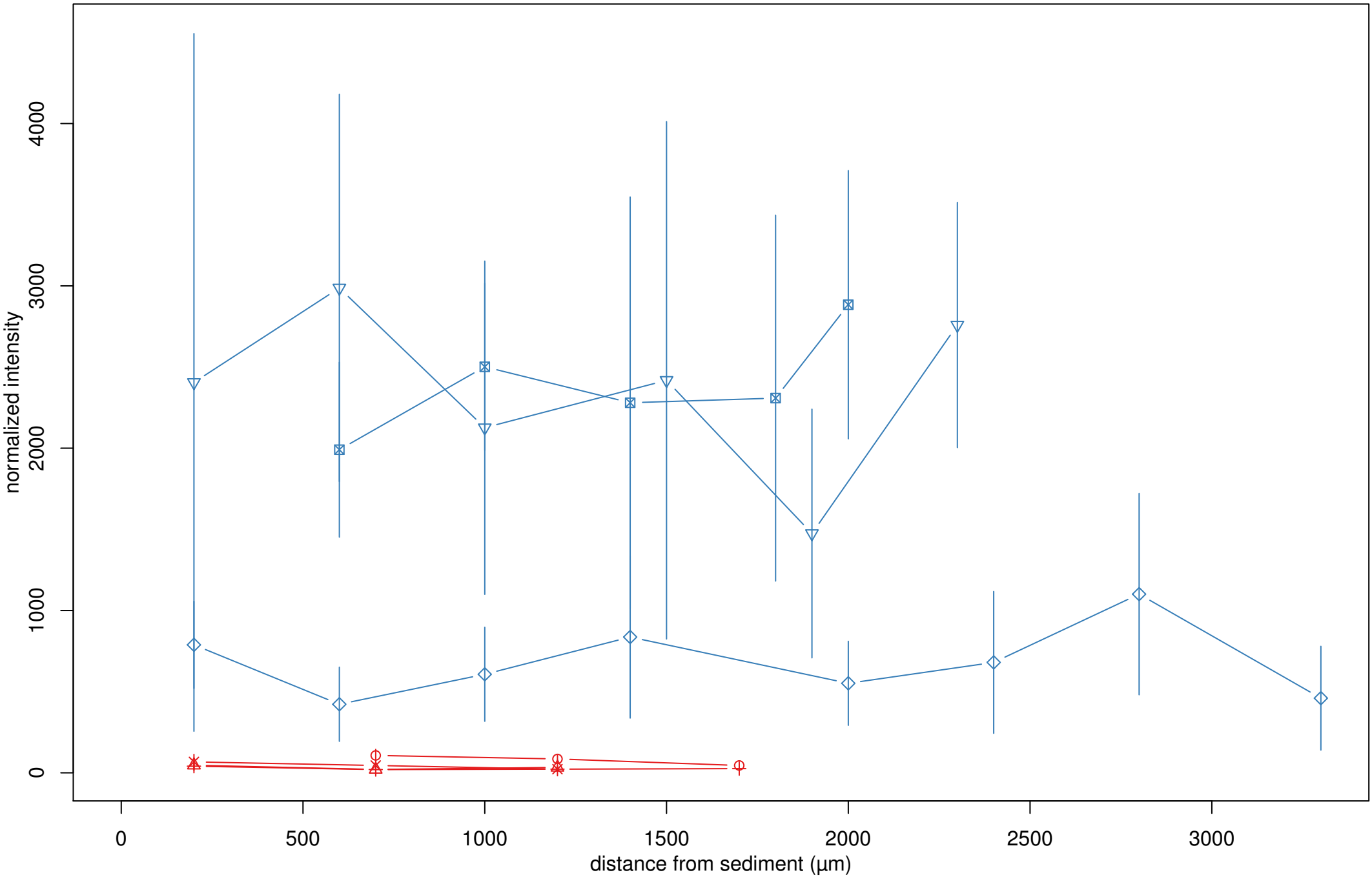
normalized intensity
0
1000
2000
3000
4000
0
500
1000
1500
2000
2500
3000
distance from sediment (µm)